Available online at www.sciencedirect.com
ScienceDirect
Journal of Power Sources 168 (2007) 391–399
JOURNAL OF POWER SOURCES
www.elsevier.com/locate/jpowsour

Fuel cell cathode air filters: Methodologies for design and optimization

Daniel M. Kennedy [a], Donald R. Cahela [a], Wenhua H. Zhu [a], Kenneth C. Westrom [b], R. Mark Nelms [b], Bruce J. Tatarchuk [a,*]

[a] *Center for Microfibrous Materials Manufacturing, Department of Chemical Engineering, Auburn University, AL 36849, USA*
[b] *Department of Electrical and Computer Engineering, Auburn University, AL 36849, USA*

Received 14 December 2006; received in revised form 8 March 2007; accepted 9 March 2007
Available online 19 April 2007

Abstract

Proton exchange membrane (PEM) fuel cells experience performance degradation, such as reduction in efficiency and life, as a result of poisoning of platinum catalysts by airborne contaminants. Research on these contaminant effects suggests that the best possible solution to allowing fuel cells to operate in contaminated environments is by filtration of the harmful contaminants from the cathode air. A cathode air filter design methodology was created that connects properties of cathode air stream, filter design options, and filter footprint, to a set of adsorptive filter parameters that must be optimized to efficiently operate the fuel cell. Filter optimization requires a study of the trade off between two causal factors of power loss: first, a reduction in power production due to poisoning of the platinum catalyst by chemical contaminants and second, an increase in power requirements to operate the air compressor with a larger pressure drop from additional contaminant filtration. The design methodology was successfully applied to a 1.2 kW fuel cell using a programmable algorithm and predictions were made about the relationships between inlet concentration, breakthrough time, filter design, pressure drop, and compressor power requirements.

Keywords: Cathode air filter; PEM stack contaminant; PEFC filter design

1. Introduction

Proton exchange membrane (PEM) fuel cells are being actively considered for a wide range of applications including automobiles, uninterruptible power supplies, and battery replacements in the military for dismounted soldiers [1]. However, air in these operating environments may contain contaminants that are damaging to fuel cell performance such as carbon monoxide, sulfur compounds, and volatile organic compounds (VOCs). It has been suggested that the best method for addressing fuel cell air contamination is by the inclusion of adsorptive filtration with a cathode air filter [2]. Filters used in PEM fuel cells must be optimized to be durable and effective, as well as easily adaptable to each specific need. Optimization of cathode filter design requires careful consideration of fuel cell operating variables and available filter technology. These design considerations were studied in detail and organized to create a process that provides a blueprint for designing and optimizing cathode air filters capable of allowing fuel cells to be operated in contaminated environments.

Research on the durability of PEM fuel cells has typically focused on the effects and the remediation of the effects of chemical contaminants on the hydrogen electrode, or anode. This focus has been driven primarily by the intent to use reformed hydrogen from fossil fuels containing contaminants toxic to the sensitive platinum catalyst. However, due to the higher complexity of the oxygen reduction reaction when compared to reduction of hydrogen at the anode, the oxygen electrode, or cathode, requires twice the platinum (0.1 mg cm^{-2} as compared to 0.05 mg cm^{-2}) and is therefore potentially more sensitive [3]. Recent studies have confirmed that polluted or otherwise contaminated environments negatively affect the performance of PEM fuel cell cathodes. For example, 20 ppm of carbon monoxide causes a temporary 4% reduction in fuel cell output. Other contaminants, for example, sulfur compounds such as H_2S and SO_2, cause a more permanent effect reducing performance to as low as 30% of original output [2,4].

Two methods for dealing with contaminated air effects on fuel cell cathodes are to increase catalyst durability and/or to filter contaminants from the air. Because of the wide variety

* Corresponding author. Tel.: +1 334 844 2023; fax: +1 334 844 2063.
E-mail address: tatarbj@auburn.edu (B.J. Tatarchuk).

0378-7753/$ – see front matter © 2007 Elsevier B.V. All rights reserved.
doi:10.1016/j.jpowsour.2007.03.020

of contaminants, increasing membrane resilience by modifying the catalyst or increasing the catalyst amount is a difficult and possibly expensive alternative. Therefore, the most effective and flexible method for operating fuel cells in contaminated environments is adsorptive filtration of contaminants from the ambient air stream.

The wide variety of filtration technology options allows for tailoring of cathode air filters to different contaminant types and concentrations. Optimization of filter design requires a methodology incorporating air properties, fuel cell attributes, and design options. A better understanding of how a cathode air filter should perform is accomplished through a detailed study of the design considerations and how they affect each other.

2. Experimental

A NEXA power module, produced by Ballard Power Systems, was used for studying compressor power relationships involving filter pressure drop. The system uses a polymer membrane electrolyte, with a platinum catalyst layer, and provides 1200 W of dc power output at a nominal output voltage of 26 V DC. Oxygen is provided to the stack by a compressor operated with a 12 V brushless dc (BLDC) motor. The compressor speed is variable, allowing for an optimized flow of air to meet system power demand.

A compressor testing apparatus was constructed to allow more control over the system. This provides a means for measuring inlet and outlet pressure, flow rate, and compressor power. Pressure was measured using a Dwyer manometer capable of measuring up to 36 in. H_2O. Flow rate was measured using an Extech hot wire anemometer at the outlet of a 3 ft long, 2 in. i.d. PVC pipe that was connected to the exit of the compressor. A motor controlling circuit was built using an ML4425 sensorless BLDC motor controller, thus allowing for power measurements to be made in dc between the power supply and controller, rather than in BLDC between the controller and the motor.

Pressure drop relationships and breakthrough data on microfibrous materials and packed beds was performed using a breakthrough testing apparatus. A constant water temperature bath was used to stabilize the concentration of hexane in bubblers. Flow rates were controlled using two rotometers, one for the flow of air through the hexane and another for the bulk flow of air into the apparatus. Concentration measurements were made using a MiniRae PID detector at the inlet and outlet of the filter. Pressure drops were measured using a Dwyer manometer, accurate up to 6 in. H_2O.

Maple Version 7.0 was used to model the final algorithm.

3. Fuel cell system design discussion and design considerations

3.1. Fuel cell system discussion

Optimization of cathode air filtration requires addressing a unique set of challenges present in the fuel cell system, shown in Fig. 1. One such challenge is how to minimize the loss in efficiency caused by chemical contaminants poisoning the cathode

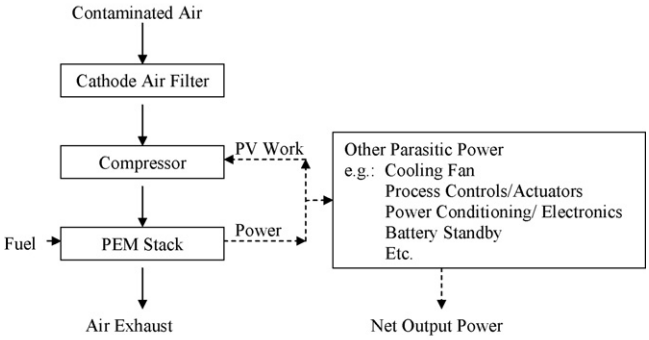

Fig. 1. Fuel cell mass and energy balance showing the flow of air and power through the system.

section catalyst. A cathode air filter can be used to remove these contaminants; however, it causes an increase in system pressure drop, presenting yet another challenge. This pressure drop causes an increase in the required amount of pressure–volume work that the compressor must perform. An energy balance must be made between the loss in power due to poisoning of the platinum catalyst and a loss in fuel cell efficiency created by an increase in parasitic power required to pump air through additional filtration.

3.2. Filter design considerations

Cathode air filter design considerations fall into six categories: inlet air properties, adsorptive filter parameters, compressor attributes, stack attributes, filter footprint, and filter design options. Fig. 2 shows how the design considerations are further broken down into individual variables within the filter and fuel cell system.

From this methodology, there are three categories of variables to consider: inlet air properties, filter design options, and filter footprint. Each of these categories can be further broken down into individual variables which can be studied for its effect on the compressor, stack, and ultimately the overall fuel cell performance. The effects of each of these categories are tied

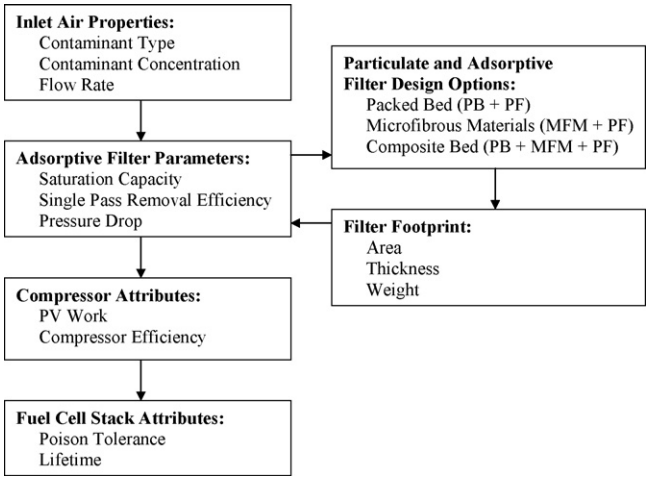

Fig. 2. Hierarchal design considerations for cathode air filters.

together with the adsorptive filter parameters: saturation capacity, removal efficiency, and pressure drop. These parameters then influence the PV work required to operate the compressor at the desired air flow rate and the stack efficiency defined by the poison tolerance and lifetime.

3.2.1. Inlet air properties

The inlet air properties, along with the stack attributes, dictate the efficacy and capability that the filters must possess. Air properties affect filter parameters by defining the capacity and removal efficiency needed to remove contaminants to achieve a specified output level. Single pass removal efficiency is increased by reducing adsorbent particle size thereby increasing surface area and eliminating intra-particle mass transport. High single pass removal efficiency results in a filter effective at removal of contaminates at low concentrations. An increase in either the capacity or the removal efficiency results in an increase in both filter pressure drop and the amount of power required by the compressor.

3.2.2. Filter design options

While many filter design options exist, for this research three options are considered: packed bed (PB), microfibrous materials (MFM), and composite bed (MFM + PB). A packed bed is the most widely used form of filtration. Packed bed characteristics include high sorbent capacity, low single pass removal efficiency, and low pressure drop. The second design option, microfibrous materials, has been proven effective with high log and high single pass removal of chemical contaminants, but has a lower capacity and higher pressure drop when compared to packed beds. Microfibrous materials also add a new dimension to the problem, through application as a pleated filter media, or as a polishing sorbent in a composite bed formation [5]. Pleated microfibrous materials have an increased capacity and lower pressure drop than a flat sheet with a smaller area. A composite bed effectively combines the capacity of a packed bed and the high contacting efficiency of microfibrous materials. An optimized composite bed is capable of higher logs of removal, has a reduced total bed depth, and has a lower pressure drop than a packed bed.

3.2.3. Filter footprint

Another category that needs to be considered for its effect on filter parameters is the filter footprint. An increase in area allows for a decrease in thickness and visa versa. In many cases, the footprint may be set by the fuel cell system in order for the filter to be retrofitted into the existing particulate filter slot. Filter weight affects the filter capacity and is required for analysis because of the differences in densities of the filter design options.

3.2.4. Adsorptive filter parameters

Inlet air properties, filter design options, and filter footprint all relate to the adsorptive filter parameters. Contaminant type, concentration, and flow rate affect the filter parameters by virtue of the differences in chemical properties that various contaminants have in relation to the filter adsorptive materials. Filter design options control the mass and energy transport properties of the filter by affecting contacting regimes as well as pressure drop. Lastly, the filter footprint affects all three filter parameters through bulk design.

3.2.5. Compressor attributes

Once the adsorptive filter parameters have been established, their effect on the compressor can be established. Pressure drop across the filter causes a decrease in inlet pressure (P_1) to the compressor creating a vacuum. The outlet pressure (P_2) from the compressor is set by the required flow rate necessary to operate the fuel cell. This increase in pressure ratio (P_2/P_1) across the compressor causes a decrease in compressor efficiency and an increase in compressor power. Both of these effects cause an overall decrease in fuel cell operating efficiency and performance.

3.2.6. Fuel cell stack attributes

The fuel cell stack is also affected by variations in the filter parameters. The stack has a certain tolerance and operating lifetime related to the concentration of contaminants passing through the cathodes of the cells. The filter controls this concentration by reducing the contaminant concentrations before they make contact with the cathode. The single pass removal efficiency required is dictated by the maximum concentration tolerable by the fuel cell. The maximum concentration may be lower if the contaminant collects in the stack rather than passing through the exhaust.

3.3. Cathode air filter optimization: a trade off between compressor power requirements and efficiency losses from catalysts poisoning

Research on cathode durability has concluded that the effect that contaminants have on fuel cell performance varies depending on the contaminant type and concentration, leading to three different scenarios for contaminant remediation. In the first scenario, contaminants have little to no permanent effect, and do not build up in the system, so can be ignored. For example, it may be more acceptable to allow a small percentage of contaminant through, rather than to increase filtration, thereby resulting in a higher pressure drop. An example of this would be CO, where the damaging effect is both small and temporary.

In the second scenario, contaminants need to be completely removed, because any amount of exposure to the contaminant will cause a permanent degradation of fuel cell performance. These contaminants build up in the system, causing more severe degradation with longer exposure times. For example, a cathode air filter must be capable of removing sulfur compounds such as H_2S and mustard gas ($C_4H_8Cl_2S$).

In the third scenario, contaminants must be removed to a point of maximum concentration to minimize a decrease in fuel cell performance. A decision for further removal beyond this defined maximum must take into account the effect the increase in filter pressure drop will have on the system. For example, SO_2 at concentrations of 2.5–5 ppm has a significant effect on fuel cell performance, with as much as a 50–60% reduction in fuel cell power [4]. This situation would clearly require a cathode

air filter for efficient fuel cell operation. SO_2 concentrations of lower than 0.5 ppm may be ignored completely as they have no noticeable effect [2], so a cathode air filter would not be necessary. However, at moderate concentrations, between 1 and 2 ppm, filtration design can be optimized between fuel cell performance and the effects of the increased filter pressure drop from additional filtration.

4. Design equations for describing fuel cell attributes and filter parameters

The following design equations provide mathematical relationships that relate the design considerations to each other. These sections include equations for determining the required air flow rate to meet fuel cell power requirements, breakthrough time based on capacity and adsorption efficiency, pressure drop based on thickness, and compressor power based on inlet and outlet pressures.

4.1. Fuel cell air flow requirements

The required oxygen flow rate to operate a fuel cell can be found by the number of faradays provided by a mole of oxygen. Through substitution and simplification the equation for the air flow rate [7] is derived

$$\text{Air flow rate} = 1.82 \times 10^{-2} \times \lambda \times \frac{P_e}{V_c}(\text{SLPM}) \tag{1}$$

where λ is the stoichiometric ratio defined as the total amount of oxygen flow divided by the oxygen used. A good approximation for the minimum stoichiometric ratio to operate a fuel cell is 3 moles of oxygen for each mole of oxygen required. P_e is the power output in watts and V_c is the average voltage across a cell. A value of 0.60 V can be used as an average voltage approximation if the value cannot be found through experimentation or is not given. This equation can be used for all fuel cells regardless of size as an estimate for air flow rate requirements [7].

4.2. Adsorptive filter breakthrough equations describing capacity, adsorption rate, breakthrough time, and inlet and outlet concentrations

Filter breakthrough equations are required to relate filter attributes to inlet and outlet air properties. The filter attributes include the chemical properties of sorbent capacity (N_0) and rate of adsorption (k'), and the footprint which includes area (A), thickness (L), and weight (m). Another attribute commonly used to describe filters is voidage (ε). The air properties are face velocity (v_0), inlet concentration (C_0), and outlet concentration (C_1). Several previously studied equations are effective at predicting breakthrough times for adsorbent beds.

An exact breakthrough equation for non-reversible adsorption onto a surface can be applied to a single or dual layer bed. Eq. (2), derived by Amundson [8], is based on mass balance across an adsorptive bed allowing for a time varying input concentration.

$$\frac{C}{C_0} = \frac{C_0(t-(\varepsilon z/v_0))\exp\left[\varepsilon(k/v_0)\int_0^{t-(\varepsilon z/v_0)} C_0(\eta)\,\mathrm{d}\eta\right]}{\exp\left[\varepsilon(k/v_0)\int_0^{z}(N_0-n(\xi))\,\mathrm{d}\xi\right] + \exp\left[\varepsilon(k/v_0)\int_0^{t-(\varepsilon z/v_0)} C_0(\eta)\,\mathrm{d}\eta\right] - 1}, \quad t \geq \varepsilon\frac{k}{v_0} \tag{2}$$

This equation is then integrated resulting in the following equations which can be used to calculate the outlet concentration of a gas after passing through a single or double layer filter. A constant inlet concentration was used to integrate the outlet concentration of the first layer (C_1). C_1 was then inserted back into Eq. (2) and integrated with respect to time to calculate the outlet concentration of the second layer (C_2). The equations are given by

$$C_1 = \frac{C_0}{1 + (\mathrm{e}^{k_1'\tau_1} - 1)\,\mathrm{e}^{-k_1'(t-\theta_1)}} \tag{3}$$

$$C_2 = \frac{C_1[1 + \mathrm{e}^{-k_1'\tau_1}(\mathrm{e}^{k_1'(t-\theta_1-\theta_2)} - 1)]^{(k_2'/k_1')}}{(\mathrm{e}^{-k_2'\tau_2} - 1) + [1 + \mathrm{e}^{-k_1'\tau_1}(\mathrm{e}^{k_1'(t-\theta_1-\theta_2)} - 1)]^{(k_2'/k_1')}} \tag{4}$$

where $k_i' = \varepsilon_i k_i C_0$ and $\theta_i = \varepsilon_i L_i / v_0$. Another equation used to determine outlet concentration from a single layer adsorptive bed, developed by Yoon and Nelson [6] is based on probabilistic reasoning

$$C_1 = \frac{C_0}{1 + \mathrm{e}^{k'(\tau - t)}} \tag{5}$$

Eq. (5) allows for estimates to be made on the breakthrough constants used in the exact breakthrough equation. By using experimental data, a regression analysis yields values for k'. Also, from a breakthrough curve, saturation capacity (τ) in units of time can be read off at the time corresponding to $C = (1/2)C_0$. This allows for solving for capacity, N_0, in grams contaminant being removed per cm^3 sorbent, by using the following equation

$$\tau = \frac{N_0 L}{v_0 C_0} \tag{6}$$

Both the k' and N_0 can be used for a prediction of breakthrough concentration at different flow rates, inlet concentrations, and filter thicknesses. Face velocity is a function of flow rate and filter surface area. Inlet concentration and time are user inputs related to the operating environment of the fuel cell. Outlet concentration can be provided by the manufacturer or estimated based on experimental data on cathode durability.

4.3. Pressure drop relationships with filter thickness and air face velocity

Pressure drop (ΔP) has been correlated with face velocity, bed depth, viscosity (μ), void fraction, and gas density (ρ). Pressure drop through both packed beds and microfibrous beds is also related to particle diameter. However, in microfibrous beds there is an additional pressure drop related to fiber diameter. The

Ergun equation [9] is commonly used to describe flow through packed beds

$$\frac{\Delta P}{L} = 150\left(\frac{\mu v_0}{D_P^2}\right)\frac{(1-\varepsilon)^2}{\varepsilon^3} + \frac{7}{4}\left(\frac{\rho v_0^2}{D_P}\right)\frac{1-\varepsilon}{\varepsilon^3} \tag{7}$$

In order to estimate the pressure drop across microfibrous materials (a high voidage mixture of fibers and particles), the porous media permeability equation (PMP) is used to apply to beds that have porosity greater than 50%. This equation considers form drag losses which are small in low porosity material (e.g. packed beds). PMP equation for high voidage microfibrous materials

$$\frac{\Delta P}{L} = 72\left(\frac{\tau^2}{\cos^2(\Theta)}\right)\left(\frac{\mu v_0}{\varepsilon^3}\right)\left(\frac{1-\varepsilon^2}{\phi D}\right)(1+X_{\mathrm{FD}}) + 6\left(\frac{\tau^3}{\cos^3(\Theta)}\right)\left(\frac{\rho v_0^2}{2\varepsilon^3}\right)\frac{1-\varepsilon}{\phi D}\left(C_{\mathrm{f}} + \frac{C_{\mathrm{FD}}}{4}\varepsilon\right) \tag{8}$$

In addition to the variables used in the Ergun equation, the PMP equation uses tortuosity ($\tau = 1 + 0.5(1-\varepsilon)$), shape factor ($\phi$), and the angle of flow paths through the bed (Θ). The coefficient of drag is represented by C_{D} for a sphere (usually 0.6). The coefficient of friction for turbulent flow is C_{f} and the coefficient of form drag of a sphere in turbulent flow is C_{FD} ($C_{\mathrm{FD}} = C_{\mathrm{D}} - C_{\mathrm{f}}$). Values corresponding to the Ergun equation can be found by equating the PMP equation to the Ergun and modified Ergun equations [9,10].

Empirical pressure drop relationships can also be determined experimentally by recording pressure drop as a function of layer thickness and flow rate. The advantage to this method is that it is more accurate; however, it prevents correlations to be made between properties of the filter such as the effects of particle size on pressure drop. An example empirical equation is

$$P_2 - P_1 = B_1 L_1 v_0 + B_2 L_1 v_0^2 \tag{9}$$

where B_1 and B_2 are parameters fitted to pressure drop data (constants for a specific material), v_0 the face velocity and L_1 is the thickness of the layer. The second term in the equation accounts for inertial losses through the filter. An example of these types of losses would occur when studying a pleated filter. In most cases, however, the losses are small and negligible.

4.4. Compressor power and efficiency

4.4.1. Compressor power

A study of the compressor is necessary to correlate the pressure ratio and power. A simple experimental setup consists of a pressure tap on each side of the compressor, a means of adding pressure drop to each side of the compressor (e.g. orifice plates), and a controller to operate the compressor. The compressor can be operated at different flow rates and pressure ratios while power provided to the compressor is recorded. Fig. 3 shows the resulting plot for a 12 V compressor used in this study. In this case the correlation is linear and can be written in the form

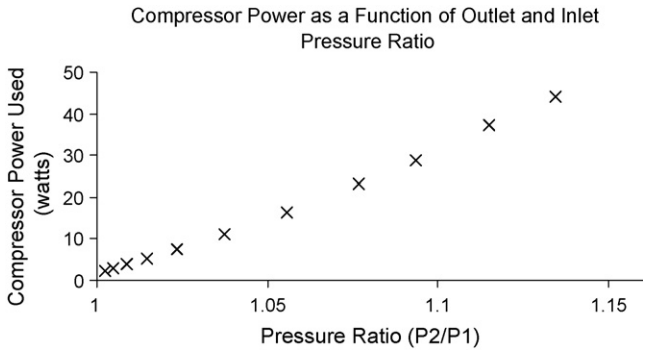

Fig. 3. Power using a 12/64 in. inlet orifice and 11/64 in. outlet orifice. Pressure ratio is increased by increasing the air flow rate.

$$\text{Compressor power} = m\left(\frac{P_2}{P_1}\right) + b \tag{10}$$

4.4.2. Compressor efficiency

Several efficiency definitions exist that can be used to describe performance of a compressor. The most common efficiency equation, due to its accuracy and ease of determining input values, is specific overall efficiency. It can be expressed

$$\bar{\eta}_{\text{overall, ad}} = \frac{\dot{m}_{\mathrm{e}} c_p T_1[(P_2/P_1)^{(k-1)/k} - 1]}{\dot{W}_{\text{shaft, e}}} \tag{11}$$

In this case, m_{e} is the experimental mass flow at the discharge, T_1 the ambient inlet temperature, P_2/P_1 the pressure ratio, and k is the constant and is 1.4 for adiabatic [7]. A compressor study that yields efficiency measurements provides the ability to locate the surge line on a performance chart, identifiable as the points where efficiency approaches zero.

4.4.3. Compressor performance charts

Another method of obtaining data on compressors is with a performance curve. Centrifugal compressors have performance charts which give the efficiency and pressure ratios at which the compressor can be operated. On this chart, efficiency is represented by constant efficiency contours. Performance charts also show a surge line, which represents the point at which the compressor becomes unstable if operated at a higher pressure ratio, at the same flow rate, or at a lower flow rate at the same pressure ratio. The surge line represents the point air flow through the compressor is unable to keep the compressor from overheating. This instability causes backflow and possible damage to the compressor. The performance chart is important in understanding the operating capabilities of the compressor, as well as to help understand power requirements [7].

5. Design algorithm

Using the previously discussed design equations and relationships, an algorithm was created to relate the design considerations to filter thickness and compressor parasitic power. The design equations were organized such that each variable could be solved starting with inputs that are readily available

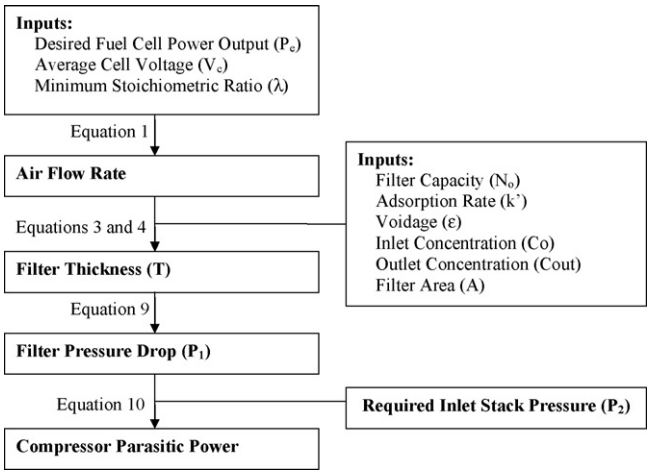

Fig. 4. Programmable design algorithm.

from the manufacturer or able to be experimentally determined. The linearity of the algorithm allows for a simple computer program to be built with few assumptions. A completed algorithm is shown in Fig. 4.

6. Design process results: application of the design algorithm to a 1.2 kW fuel cell

The cathode air filter design algorithm was applied to a 1.2 kW fuel cell in order to compare filter design options for removal of hexane with activated carbon. Hexane was used for this study because of its ease of use in the laboratory and well known adsorptive characteristics when used with activated carbon.

Four different design options were considered for this fuel cell application. The first three options were packed bed, microfibrous sheet, and composite bed. For these options a filter area of 55 cm^2 was studied for its ability to be retrofitted into the existing particulate filter location in the fuel cell when total thickness is less than 1 cm. The fourth design option, a pleated microfibrous materials filter, will be studied separate from the other filters. The pleated filter will be studied for the effects of breakthrough time and concentrations on the variable sheet thickness of the filter while the pleat depth is held constant at 1 cm, corresponding to the size required to retrofit the fuel cell.

In order to understand the effects of different inlet and outlet concentrations on the optimum filter designs, three case scenarios were studied. The three cases were:

Case I: 100–5 ppm.
Case II: 10–0.1 ppm.
Case III: 100–0.1 ppm.

Values shown in Table 1 were used to represent the fuel cell system and were obtained from the operating fuel cell manual. The other inputs were experimentally determined. Breakthrough tests were performed on both 12–30 mesh activated carbon and a microfibrous polishing layer with a basis weight of 870 g m^{-2} with 18.3% 60–140 mesh activated carbon. Values for k' and N_0 were regressed from experimental breakthrough data using the equation provided by Yoon and Nelson. Pressure drop relationships were determined in the laboratory as a function of thickness and flow rate. All resulting data used in describing the filter options are shown in Table 2.

Table 1
Quantitative fuel attributes used in the algorithm

Input parameter	Parameter value
Fuel cell power output (P_e)	1200 W
Average cell voltage (V_c)	0.60 V
Minimum stoichiometric ratio (λ)	2.7

Table 2
Filter design input parameters collected from experimental data

Design parameter	Microfibrous layer	Packed bed
Filter capacity (N_0)	0.04 moles hexane cm^{-3}	0.1 moles hexane cm^{-3}
Adsorption rate (k')	$0.00332C_0$	$0.00183C_0$
Voidage (ε)	0.772	0.4
Air flow rate	89.5 LPM	89.5 LPM
Pressure drop	$0.0664L_2v_0$	$0.0514L_1v_0$
Compressor power	$313.14(P_2/P_1) - 312.74$	$313.14(P_2/P_1) - 312.74$

The algorithm was used to predict an optimum filter thickness and the corresponding power requirements to operate the compressor. By varying the inlet concentration, outlet concentration, and breakthrough times, the different design options were studied under different capacity requirements and removal efficiency requirements.

6.1. Case study of microfibrous layer, packed bed

For Case I, Figs. 5 and 6 show the compressor power and predicted thickness requirements for different filter configurations optimized to meet breakthrough time requirements at an inlet concentration of 100 ppm and an outlet concentration of 5 ppm. This removal represents a 1.3 log removal and requires a high filter capacity. Because of the high capacity, the packed bed represents the best solution based on total filter thickness and pressure drop/compressor power. Because of the low logs of removal, microfibrous materials were not affective in reducing thickness or power requirements and therefore provided no benefit when used alone or in conjunction with a packed bed (composite bed).

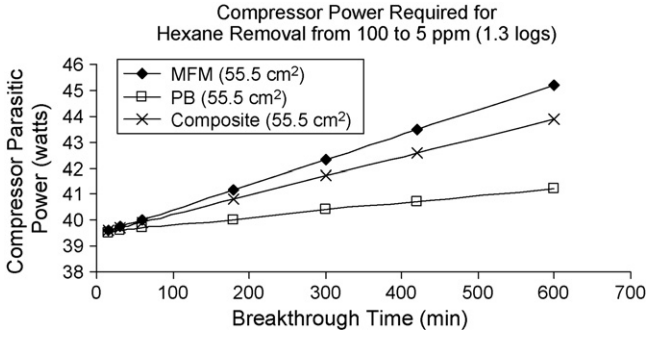

Fig. 5. Predicted power required to meet breakthrough time requirements.

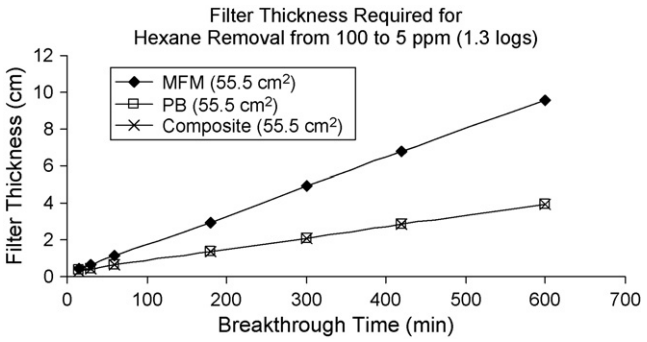

Fig. 6. Predicted thickness required to meet breakthrough time requirements.

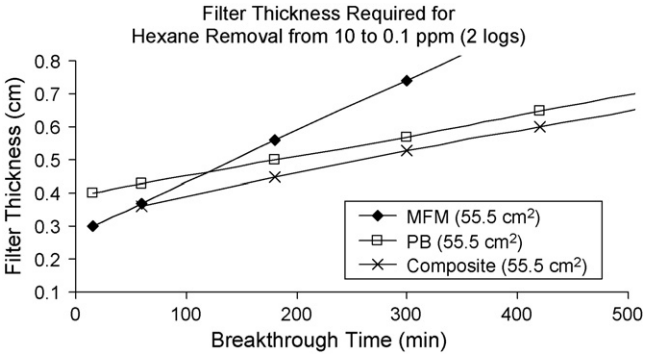

Fig. 7. Predicted thickness required to meet breakthrough time requirements.

From Fig. 7 (representing Case II), it is evident that microfibrous materials provide the thinnest filter option for a breakthrough time of less than 50 min; however, this solution also creates the most pressure drop, as evidenced by the increase in parasitic power requirements. If, in practice, power requirements are the priority, then a composite bed provides the best solution. A composite bed also provides the best solution for higher breakthrough times. Fig. 7 shows that a composite bed at the same thickness as a packed bed provides about a 100 min longer breakthrough time.

The third scenario, shown in Fig. 8, tests filter options under a situation that requires both a high capacity filter that is also capable of high logs of removal. In this situation, a composite bed outperforms the other design options by having a lower total thickness than the packed bed. It is also evident from Fig. 8 that the addition of a microfibrous layer in place of a small length

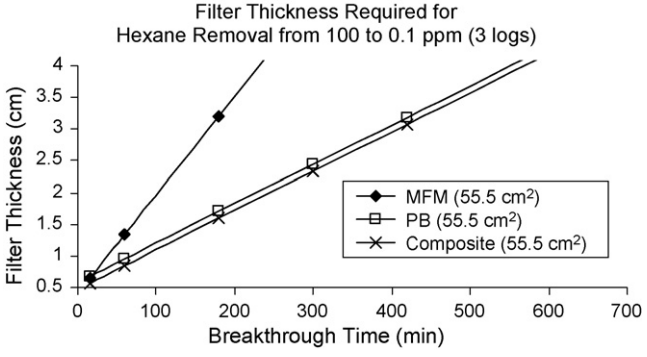

Fig. 8. Predicted thickness required to meet breakthrough time requirements.

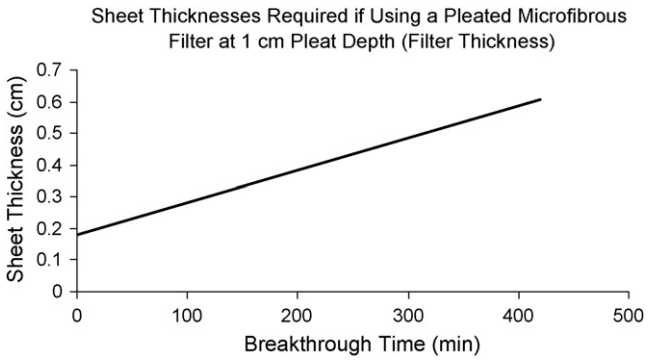

Fig. 9. Predicted sheet thickness of a microfibrous pleated filter at a challenge; concentration of 10 ppm hexane and an outlet concentration of 0.1 ppm.

of packed bed to make a composite bed causes little additional pressure drop.

6.2. Case study for a pleated microfibrous filter

For an analysis of a pleated filter as a design option, a pleat depth of 1 cm was assumed and the thickness of the sheet was variable like the previous design options. This resulted in a constant filter thickness of 1 cm even though the sheet thickness was variable. Because of the pleats, a larger surface area was able to fit into the same dimensions as the other options. A pleated microfibrous sheet was represented in the algorithm as having an area of 105.5 cm^2 (pleat factor of 1.9). This pleat factor was only attainable at layer thicknesses less than 0.5 cm if it is still to fit in the 1 cm pleat depth, and will only be studied up to that thickness.

Fig. 9 shows the sheet thickness power requirements if a pleated filter is used. The filter was only studied at an inlet concentration of 10 ppm and an outlet concentration of 1 ppm. The breakthrough time can be greatly prolonged by reducing the inlet poison concentration. If C_0 is changed from 10 to 0.5 ppm for a breakthrough concentration of 0.1 ppm at the outlet, the breakthrough time is approximately increased from 300 to 6000 min (100 h). For the application of fuel cells, the environmental poison concentration is relatively low, and the breakthrough time will be much longer than in the laboratory test condition. An increase in sheet thickness results in only a small percentage increase in compressor power requirements from additional pressure drop. Pleated filters provide an additional solution for low capacity, high log removal applications. Another advantage to using a pleated filter rather than a packed or composite bed is the stability from the sinter locked network which adds resilience to the filter.

6.3. Detailed composite bed configuration analysis

For each case study and each breakthrough time tested, the composite bed was optimized to minimize total bed depth. This was accomplished by varying the thickness of the packed bed, calculating the required thickness of the microfibrous layer, and calculating the total thickness. Table 3 shows the individual layer thicknesses for each of the breakthrough times in the case study.

Table 3
Predicted, optimized individual layer thicknesses of the packed bed (L_1) and microfibrous layer (L_2) used to create a composite bed

Time (min)	Case I		Case II		Case III	
	100–5 ppm (1.3 logs removal)		10–0.1 ppm (2 logs removal)		100–0.1 ppm (3 logs removal)	
	L_1 (cm)	L_2 (cm)	L_1 (cm)	L_2 (cm)	L_1 (cm)	L_2 (cm)
15	0.2	0.12	N/A	N/A	0.2	0.37
60	0.52	0.09	0.09	0.27	0.51	0.34
180	1.26	0.09	0.23	0.22	1.25	0.34
300	2	0.09	0.32	0.21	2	0.34
420	2.74	0.09	0.4	0.2	2.74	0.34
600	3.86	0.09	0.5	0.2	3.85	0.34
6000	37.29	0.09	3.86	0.2	37.28	0.34

By studying these graphs, information can be learned about the capacity and removal efficiency requirements of the filter and how filter configurations are affected by inlet concentration, outlet concentration, and breakthrough time.

Cases I and III require the thickest packed bed portion due to the fact that they have the higher capacity requirements of 95 and 99.9 ppm removal, respectively, when compared 9.9 ppm removal requirement for Case II. Secondly, the thickness of the microfibrous layer increases with log removal requirements. This is a result of the higher single pass removal efficiency required for high log removal.

Further analysis is performed by moving down the columns and considering higher breakthrough time requirements. By increasing breakthrough time, additional capacity is required to meet the breakthrough requirements. This results in an increase in the thickness of the packed bed layer of the filter. However, at low breakthrough times, where capacity is less significant, a thicker microfibrous layer provides a shorter overall bed depth by reducing the critical bed depth (the minimum bed depth required to prevent immediate breakthrough).

7. Filter tests results

7.1. Composite bed filter

Fig. 10 shows the results of the 100 ppm challenge breakthrough test on the composite bed filter. Breakthrough at 0.1 ppm was 27 min. Predicted value was 100 min. The predicted curve shows a sharper breakthrough. A shallower breakthrough curve results from a lower contacting efficiency than predicted. Since contacting efficiency is primarily a factor of adsorption rates the inaccuracy in the breakthrough curve is caused by inaccuracy in the determination of the adsorption rate values. The filter capacity is only slightly overestimated by the algorithm and as a result the breakthrough is sooner than predicted.

Pressure drop predictions, shown in Fig. 11, were accurate at flow rates lower than 70 SLPM when compared to experimentally determined data. At higher flow rates actual pressure drop was higher than predicted. This may be due to inertial losses which cause a non-linear pressure drop relationship when operating at higher flow rates and was assumed negligible when the pressure drop formula was determined for a packed bed.

7.2. Pleated microfibrous filter

Fig. 12 shows breakthrough curves predicted by the algorithm compared with those found experimentally. In this case, the breakthrough was 15 min sooner than predicted, indicating that the capacity was overestimated. Adsorption rate values were more accurate, evident by the similar shape of the sigmoidal breakthrough curve for both the actual and predicted curves. Pressure drop predictions for the pleated filter, shown in Fig. 13, are higher than actual values. A small percentage of this difference in pressure drop is a result of leaks in the filter and can be resolved with better construction techniques. A small curvature in the actual pressure drop is the result of inertial losses due to the air having to pass through the pleats. Inertial losses were

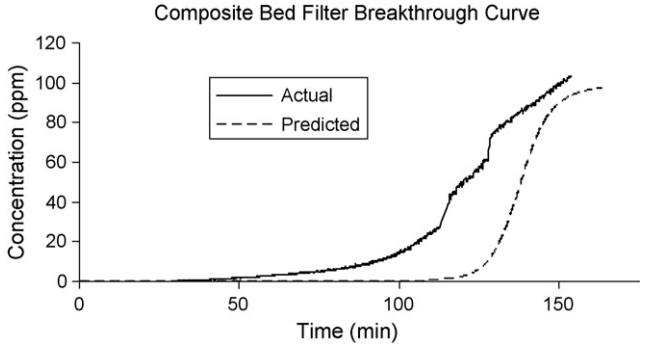

Fig. 10. Actual breakthrough curves for composite bed compared to a predicted breakthrough curve by the algorithm.

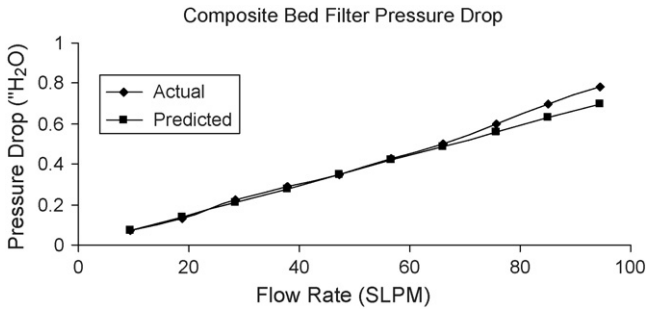

Fig. 11. Pressure drop comparison between a composite bed filter and values predicted by the algorithm.

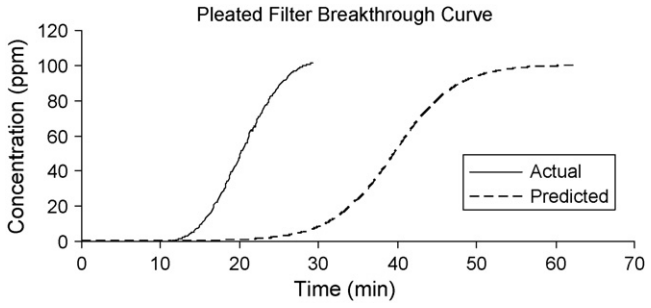

Fig. 12. Actual breakthrough curves for a pleated filter compared to a predicted breakthrough curve by the algorithm.

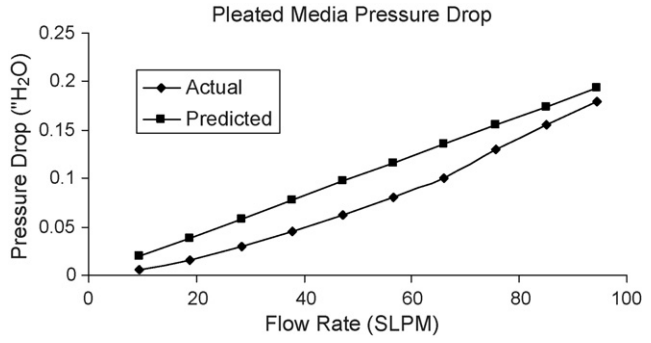

Fig. 13. Pressure drop comparison between a microfibrous pleated filter and values predicted by the algorithm.

assumed negligible in original pressure drop calculations used to predict the pressure drop; therefore, the predictions were less accurate.

8. Summary and conclusions

Optimization of a cathode air filter design to a variety of different fuel cell applications involves inputting design considerations into an algorithm predicting compressor power and filter breakthrough characteristics, both of which reflect fuel cell performance and net power output. Results from application of a programmable design algorithm to a 1.2 kW fuel cell show that the algorithm and design methodology are effective means of predicting filter effects on compressor power requirements. The predictions also show trends useful in tailoring a filter to specific requirements of an application.

Microfibrous materials provide the lowest pressure drop for cases requiring high log removal due to their high contacting efficiency. Packed beds have the lowest pressure drop for applications requiring a high capacity. However, the bed depth of a packed bed becomes large when meeting high log removal requirements. An optimized composite bed provides the most favorable solution for cases requiring both high contacting efficiency and high capacity. A filter must be optimized for each contaminant type and concentration to achieve the required operating life of the fuel cell and to minimize pressure drop which can consume as much as 1% of total output power. Use of a design algorithm provides a means of optimization by comparing the effectiveness of different filter configurations, ultimately yielding higher fuel cell efficiency and operating life.

References

[1] J.M. Moore, J.B. Lakeman, G.O. Mepsted, J. Power Sources 106 (2002) 16–20.
[2] J.M. Moore, P.L. Adcock, J.B. Lakeman, G.O. Mepsted, J. Power Sources 85 (2000) 254–260.
[3] P. Costamagna, S. Srinivasan, J. Power Sources 102 (2001) 242–252.
[4] R. Mohtadi, W. Lee, J.W. Van Zee, J. Power Sources 138 (2004) 216–225.
[5] D.R. Cahela, B.J. Tatarchuk, Proceedings of the AIChE 2003 Annual Meeting, November 16–21, 2003: Fundamentals of Adsorption and Ion Exchange II, San Francisco, CA, 2003.
[6] Y.H. Yoon, J.H. Nelson, Am. Ind. Hyg. Assoc. J. 45 (1984) 509.
[7] J. Larminie, A. Dicks, Fuel Cell Systems Explained, second ed., SAE International, May 2003 (Chapter 1 and Appendix A 2.2).
[8] N.R. Amundson, J. Phys. Colloid Chem. 52 (1948) 1153–1157.
[9] D.R. Cahela, B.J. Tatarchuk, Catal. Today 69 (2001) 33–39.
[10] D.K. Harris, D.R. Cahela, B.J. Tatarchuk, Composites: Part A 32 (2001) 1117–1126.